[14]J. Ziman, Ref. 12, p. 257.
[15]J. Ziman, Ref. 12, p. 412.
[16]J. Ziman, Ref. 12, p. 129.
[17]F. J. Blatt and H. R. Fankhauser, Phys. Kondensierten Materie 3, 183 (1965).
[18]D. K. C. McDonald, *Thermoelectricity* (Wiley, New York, 1962), p. 107.
[19]In a few exceptional situations S^T_{pho} may be slightly positive at extremely low temperatures.
[20]Except at very low temperatures where it may undergo one or two sign changes.
[21]R. L. Carter, A. I. Davidson, and P. A. Schroeder, J. Phys. Chem. Solids (to be published).
[22]N. Cusack and P. Kendall, Proc. Phys. Soc. (London) 72, 898 (1958).
[23]G. Borelius, *Handbuch der Metallphysik*, edited by G. Masing (Akademische Verlagsgesellschaft, Leipzig, 1935), p. 185.
[24]H. J. Trodahl, Rev. Sci. Instr. 40, 648 (1969), see particularly Fig. 7.
[25]Ch. Kittel, *Introduction to Solid State Physics* (Wiley, New York, 1966).
[26]J. J. Vuillemin, Phys. Rev. 144, 396 (1966).
[27]T. Aisaka and M. Shimizu, J. Phys. Soc. Japan 28, 646 (1970).
[28]M. V. Vedernikov, Advan. Phys. 18, 337 (1969).
[29]D. Bierens de Haan, *Nouvelles Tables d'Integrales Définies* (Hafner, New York, 1939), p. 148.
[30]H. B. Dwight, *Tables of Integrals and other Mathematical Data*, 4th ed. (MacMillan, New York, 1965), p. 30.

PHYSICAL REVIEW B VOLUME 4, NUMBER 2 15 JULY 1971

Effect of Fermi Surface Geometry on Electron-Electron Scattering*

Christopher Hodges
Queens University, Kingston, Ontario, Canada

and

Henrik Smith
Physics Laboratory I, *H. C. Ørsted Institute, Universitetsparken* 5, *Copenhagen Ø., Denmark*

and

J. W. Wilkins†
Laboratory of Atomic and Solid State Physics, Cornell University, Ithaca, New York 14850
(Received 5 November 1971)

In order to investigate the influence of Fermi-surface geometry on the lifetime of an electron due to interactions with other electrons, we have performed a calculation (using Fermi's "Golden Rule")of the energy- and temperature-dependent lifetime of an electron on a cylindrical Fermi surface. At zero temperature, the dominant energy dependence of the inverse lifetime or the decay rate is $\epsilon^2|\ln\epsilon|$ for small values of the parameter ϵ which is the electron energy relative to the Fermi energy μ measured in units of μ. At finite temperatures the decay rate leads to an electrical resistivity proportional to $T^2|\ln kT/\mu|$ instead of the T^2 dependence characteristic of a spherical Fermi surface. In addition, the similar calculation (using Fermi's "Golden Rule") for a spherical Fermi surface has been done exactly at zero temperature. The magnitude of the correction to the well-known ϵ^2 term has been obtained. Furthermore, in an appendix, written with N. D. Mermin, the dominating influence of the density of states on the wave-vector dependence of the susceptibility is demonstrated.

I. INTRODUCTION

The possibility of observing the contribution of electron-electron scattering to the resistivity of metals is a subject of much current experimental and theoretical interest. [1] In the analysis of experimental data such scattering processes have usually been assumed to contribute a term proportional to T^2 in the resistivity. The rationale for this is the well-known result [2] that the rate of decay due to electron-electron interactions of an electron in state $\vec{p}_1$ with energy ϵ_1 (measured from the Fermi energy μ) is proportional to $[(\pi kT)^2+\epsilon_1^2]$, when the Fermi surface is *spherical*. Such a rate of decay causes a resistivity proportional to T^2 provided a mechanism for degradation of the total momentum exists. This energy and temperature dependence of the decay rate is derived on the assumption that $kT \ll \mu$ and $\epsilon_1 \ll \mu$, which is also the region of interest in the present investigation.

In this paper we report a calculation of the energy and temperature dependence of the decay rate of an electron on a *cylindrical* Fermi surface in order to illustrate the effect of geometry on the availability of phase space for the scattering. The cylindrical geometry is supposed to arise from a band-structure calculation that gives one-electron energies $\epsilon_p = p^2/2m$, where p is the magnitude of the compo-

nent of the momentum perpendicular to the cylinder axis.

We find that the rate of decay in the cylindrical case is dominated by a term proportional to $T^2|\ln kT/\mu|$ rather than T^2. In metals with cylindrical pieces of Fermi surface one would consequently expect the electron-electron scattering on the cylindrical pieces to contribute a term proportional to $T^2|\ln kT/\mu|$ to the resistivity.

It is frequently[3] argued that the contribution of electron-electron scattering to the resistivity is proportional to T^2, since the temperature dependence of the decay rate arises from the need for satisfying the exclusion principle twice. This introduces two factors of (kT/μ) in the decay rate, since (kT/μ) denotes the fraction of the total number of electrons that can undergo scattering. Our result for the cylindrical geometry shows the limitations of this argument and demonstrates in a specific example the effect of a nonspherical geometry.

One reason for expecting the decay rate on a cylindrical surface to differ from that on a spherical surface is the observation that the two-dimensional density of states for noninteracting electrons is independent of energy, whereas the three-dimensional one depends on the square root of the energy. This difference between the cylinder and the sphere can be shown to affect a quantity such as the static wave-vector-dependent susceptibility $\chi(q)$. For noninteracting electrons occupying a cylindrical Fermi sea, $\chi(q)$ turns out (Appendix A) to be constant for q (perpendicular to the axis of the cylinder) less than the diameter of the cylinder and only starts to decrease when q exceeds that value.[4] By contrast, the static susceptibility for a sphere of noninteracting electrons decreases monotonically with q as q goes from zero to infinity.

The plan of the paper is as follows: In Sec. II we calculate the decay rate in the cylindrical geometry by Fermi's "Golden Rule" keeping terms proportional to $T^2|\ln kT/\mu|$ as well as terms proportional to T^2. In Appendix A the static susceptibility of a cylindrical Fermi sea of noninteracting electrons is discussed in detail. A useful relation between coordinates is dealt with in Appendix B and the evaluation of a certain integral is discussed in Appendix C. Finally, Appendix D demonstrates another way of calculating the decay rate via the frequency-dependent susceptibility function, and contains the result of an exact calculation of the decay rate on a spherical surface by this method.

II. DECAY RATE AT $T \neq 0\,^\circ$K

Our consideration of the decay rate of an electron on a cylindrical Fermi surface starts from the usual expression[2]

$$\frac{1}{\tau(\vec{p}_1)} = \sum_{\vec{p}_{1'}} \sum_{\vec{p}_{2'}} \int d\vec{p}_2\, W(1-f_{\vec{p}_{1'}}) f_{\vec{p}_2}(1-f_{\vec{p}_{2'}}) \times \delta(\vec{p}_1+\vec{p}_2-\vec{p}_{1'}-\vec{p}_{2'})\, \delta(\epsilon_1+\epsilon_2-\epsilon_{1'}-\epsilon_{2'}), \quad (1)$$

which is the rate of decay of an electron in state $\vec{p}_1$ due to the collision process $(\vec{p}_1, \vec{p}_2) \rightarrow (\vec{p}_{1'}, \vec{p}_{2'})$. The δ functions assure conservation of momentum and energy in the electron-electron collision. The transition probability is W [which is equal to $(2\pi/\hbar)|V_{\vec{p}_1,\vec{p}_{1'}}|^2$ in the Born approximation, $V_{\vec{p}_1,\vec{p}_{1'}}$ being the matrix element of the scattering potential]. We shall treat W as a constant in the following. Provided W tends towards a constant at small values of the momentum transfer in the collision, one can neglect the momentum dependence of W, as discussed in Appendix E.[5] However, the Fermi factors $f_{\vec{p}}$ depend strongly on energy and cause the dominant temperature and energy dependence of $1/\tau$.

The Fermi sea is a cylinder of length L, which means that the energies, and hence the Fermi factors, depend only on the components of the momenta perpendicular to the cylinder axis. It is therefore very convenient to introduce cylindrical coordinates.

In (1) we may change the sums over phase space into integrals and then remove three of the nine integrations over components of momenta by virtue of the momentum-conserving δ function. The result is

$$\frac{1}{\tau(\epsilon_1)} = 2\frac{W}{(2\pi\hbar)^6} \int d^3p_{1'} \int d^3p_2 (1-f_{\vec{p}_{1'}}) \times f_{\vec{p}_2}(1-f_{\vec{p}_2+\vec{p}_1-\vec{p}_{1'}})\, \delta(\epsilon_1+\epsilon_2-\epsilon_{1'}-\epsilon_{2'}), \quad (2)$$

where the factor of 2 arises from spin considerations. Furthermore, we have used the assumption of a constant W. Note that in (2) $\epsilon_{2'} = (1/2m) \times (\vec{p}_1+\vec{p}_2-\vec{p}_{1'})^2$.

We now introduce cylindrical coordinates

$$d^3p_{1'} = p_{1'}\, dp_{1'}\, d\theta_{1'}\, dq_{1'}\,, \qquad d^3p_2 = p_2 dp_2\, d\theta_2\, dq_2\,. \quad (3)$$

The azimuthal angles are measured with respect to $\vec{p}_1$. The q's are the components of momentum along the axis of the cylinder. In (2) neither the Fermi functions nor the energy δ function depend on the q's. Consequently, we may take all four momenta to lie in the same plane perpendicular to the cylindrical axis (Fig. 1).

We first integrate over $\theta_{1'}$, keeping $p_{1'}$, p_2, and θ_2 constant. Therefore, in the energy-conserving δ function only $\epsilon_{2'}$ depends on $\theta_{1'}$. We may then write

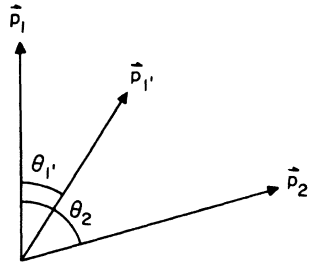

FIG. 1. The relevant angles between the components of the momenta perpendicular to the cylinder axis [cf. Eq. (3) and Appendix B].

$$\delta(\epsilon_1+\epsilon_2-\epsilon_{1'}-\epsilon_{2'})=\left|\frac{\partial\epsilon_{2'}}{\partial\theta_{1'}}\right|^{-1}_{\theta_{1'}=\theta_{1'_0}}\delta(\theta_{1'}-\theta_{1'_0}), \tag{4}$$

where $\theta_{1'_0}$ is determined by the zero of the energy δ function. In Appendix B we determine $\theta_{1'_0}$ and

$$\left|\frac{\partial\epsilon_{2'}}{\partial\theta_{1'}}\right|_{\theta_{1'}=\theta_{1'_0}},$$

using conservation of energy and momentum. The result is

$$\left|\frac{\partial\epsilon_{2'}}{\partial\theta_{1'}}\right|_{\theta_{1'}=\theta_{1'_0}}=2[(\epsilon_{1'}-\epsilon_2)(\epsilon_1-\epsilon_{1'})+(\mu+\epsilon_1)(\mu+\epsilon_2)\sin^2\theta_2]^{1/2}, \tag{5}$$

where all energies are measured from the Fermi energy μ. The condition that the quantity under the square-root sign of (5) be positive or zero puts a constraint on the integration over θ_2. In (5) we may furthermore approximate $(\mu+\epsilon_1)(\mu+\epsilon_2)$ by μ^2. This only affects terms of higher order in (kT/μ) or (ϵ_1/μ) rather than the $T^2|\ln kT/\mu|$ and T^2 terms we are after. With the definitions

$$t\equiv\epsilon_1/kT,\quad x\equiv\epsilon_{1'}/kT,\quad \text{and } z\equiv\epsilon_2/kT,$$

after integrating over $q_{1'}$, q_2, and $\theta_{1'}$ and using $d\epsilon_{1'}=(p_{1'}/m)\,dp_{1'}$ and $d\epsilon_2=(p_2/m)\,dp_2$, we finally obtain

$$\frac{1}{\tau(t)}=\frac{2W}{(2\pi\hbar)\mu^6}\,m^2L^2(kT)^2\,2\int_{-\infty}^{\infty}dx\int_{-\infty}^{\infty}dz\times f(z)\,[1-f(x)]\,[1-f(t+z-x)]\,I(A), \tag{6}$$

where $f(x)=(e^x+1)^{-1}$ and $I(A)$ is defined in (7) and (8) below. The integrations over x and z have been extended to minus infinity. The angular integral $I(A)$, where

$$A=(kT/\mu)^2\,(x-z)\,(t-z) \tag{7}$$

is given by

$$I(A)=\frac{1}{2}\int_{\theta_0}^{\pi-\theta_0}d\theta_2\,(A+\sin^2\theta_2)^{-1/2}=\int_{u_0}^{1}\frac{du}{(1-u^2)^{1/2}(A+u^2)^{1/2}}, \tag{8}$$

where the second equality follows from the substitution $u=\sin\theta_2$. The lower limit for u is

$$u_0=\sin\theta_0=\begin{cases}0, & A>0\\ |A|^{1/2}, & A<0.\end{cases}$$

When $kT\ll\mu$, the quantity A is small and the elliptic integral (8) is approximately

$$I(A)\simeq\ln 4-\ln|A| \tag{9}$$

for both positive and negative A. The first correction to (9) is proportional to $(kT/\mu)^2$ and gives rise to a term of order $T^4|\ln kT/\mu|$.

The insertion of (9) into (6) together with the identity

$$\int_{-\infty}^{\infty}dx\int_{-\infty}^{\infty}dz f(z)\,[1-f(x)]\,[1-f(t+z-x)]=\tfrac{1}{2}(\pi^2+t^2)\,[1-f(t)] \tag{10}$$

allows us to write (6) in the form

$$\frac{1}{\tau(t)}=\frac{4L^2m^2W}{(2\pi\hbar)^6\mu}\,(kT)^2\,[1-f(t)]\times[\tfrac{1}{2}(\ln 4+|\ln kT/\mu|)(\pi^2+t^2)-F(t)], \tag{11}$$

where

$$F(t)=[1-f(t)]^{-1}\,\tfrac{1}{2}\int_{-\infty}^{\infty}dx\int_{-\infty}^{\infty}dz\ln|(x-z)(t-x)|\times f(z)\,[1-f(x)]\,[1-f(t+z-x)]. \tag{12}$$

The evaluation of (12) is discussed in Appendix C. The function $F(t)$ is even in t and equal to 0.41 for $t=0$. The range of interest is that in which $-\partial f/\partial t$ is appreciable [see Eq. (13) below]. The variation with t of $F(t)$ over the range of interest is shown in Fig. 2 and compared with the function $(\ln 2)\,(\pi^2+t^2)$ appearing in (11). It is evident that the former contribution to the T^2 term of $1/\tau(t)$ is numerically smaller than the latter in the range of interest ($t\lesssim 4$). We therefore conclude from (11) that the $T^2|\ln kT/\mu|$ term in $1/\tau(t)$ dominates the T^2 term as long as μ/kT is large compared to 4.

The transport relaxation time that enters into a calculation of the resistivity is not $\tau(t)$ itself, but rather $\tau(t)\,[1-f(t)]$, which is the reason we have taken out the factor $[1-f(t)]$ in $1/\tau(t)$. If we neglect the scattering into the beam in the manner of Herring [6] the temperature dependence of the resistivity ρ obtained from (11) is given by

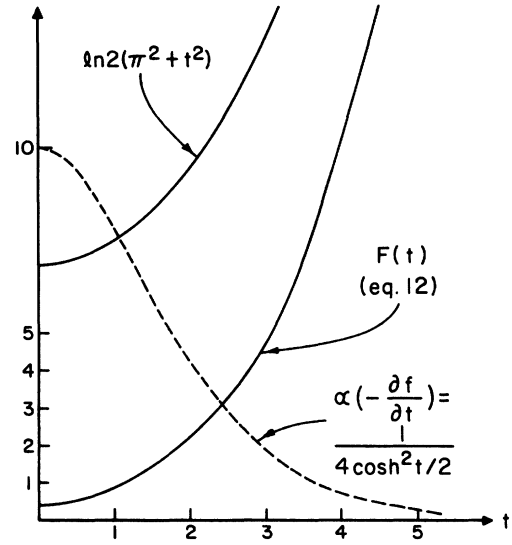

Fig. 2. The solid curves show the magnitude of the T^2 contributions to $1/\tau(t)$ as given in (12). When $t \to \infty$ the leading term of $F(t)$ equals $\frac{1}{2}t^2 \ln t$. Note that $\ln 2(\pi^2+t^2)$ dominates $F(t)$ in the range of interest ($t \lesssim 4$) where $-\partial f/\partial t$ is appreciable (indicated by the dashed line).

$$\frac{1}{\rho} \propto \int_{-\infty}^{\infty} \left(-\frac{\partial f}{\partial t}\right) \tau(t)\,[1-f(t)]\,dt. \tag{13}$$

Upon neglect of the terms in $1/\tau(t)$ proportional to T^2, the resistivity deduced from (11) and (13) becomes

$$\rho \propto T^2 \left|\ln kT/\mu\right|. \tag{14}$$

According to the discussion following Eq. (12), the result (14) is valid for $\mu/kT \gg 4$, which is easily satisfied under normal experimental conditions.

III. DECAY RATE AT ZERO TEMPERATURE

The calculation of the decay rate is somewhat simpler at zero temperature, since the Fermi factors are then step functions. The expression (6) for the decay rate is therefore replaced by the following:

$$\frac{1}{\tau(\epsilon_1)} = 2\frac{L^2m^2W}{(2\pi\hbar)^6}\,\frac{\mu^2}{2\mu}\,2 \times \int_0^{\pi} d\theta_2 \int_0^{\infty} dx \int_{-\infty}^{0} dy\, \frac{\theta(\epsilon - x + y)}{[(x-y)(\epsilon - x) + \sin^2\theta_2]^{1/2}}\,, \tag{15}$$

where energies are now measured in units of the Fermi energy μ rather than kT, that is, $x \equiv \epsilon_1/\mu$, $\epsilon \equiv \epsilon_1/\mu$, and $y \equiv \epsilon_2/\mu$. Since $(x-y)(\epsilon - x)$ is never negative, the lower limit on θ_2 is 0.

Letting $y \to -y$ and introducing a new variable $z = \epsilon - x$ we find as before the terms which dominate as $\epsilon \to 0$. To terms of order $\epsilon^2|\ln\epsilon|$ and ϵ^2 the energy dependence of (15) is

$$I(\epsilon) \equiv \int_0^{\infty} dx \int_0^{\infty} dy \int_0^1 \frac{du}{(1-u^2)^{1/2}}\,\frac{\theta(\epsilon - x - y)}{[(x+y)(\epsilon - x) + u^2]^{1/2}}$$

$$\simeq -\frac{1}{2}\int_0^{\epsilon} dz \int_0^{z} dy\, \ln[z(\epsilon + y - z)] + (\ln 4)\,(\tfrac{1}{2}\epsilon^2)$$

$$= (-\tfrac{1}{2}\ln\epsilon + \tfrac{1}{4} + \ln 2)\,\epsilon^2. \tag{16}$$

The decay rate (15) then becomes

$$\frac{1}{\tau(\epsilon_1)} = 4\,\frac{L^2m^2W}{\mu(2\pi\hbar)^6}\left[+\frac{1}{4} + \ln 2 + \frac{1}{2}\left|\ln\frac{\epsilon_1}{\mu}\right|\right]\epsilon_1^2\,. \tag{17}$$

We note from the result (17) that the characteristic $T^2|\ln kT/\mu|$ term in (11) at zero temperature is replaced by $\epsilon_1^2|\ln\epsilon_1/\mu|$ as one might reasonably expect.

The zero-temperature expression (17) can also be obtained directly from (11) by letting $T \to 0$.

IV. CONCLUDING COMMENTS

In conclusion we have found in a specific example that the effect of Fermi-surface geometry on the energy and temperature dependence of the lifetime is considerable. Whether $T^2|\ln kT/\mu|$ terms in the experimentally measured resistivity can actually be identified remains an open question. Real metals do not have Fermi surfaces which are ideally cylindrical. Palladium might be considered as a candidate. However, the open scaffold structure of Pd is for our purpose not well approximated by (intersecting) cylinders as shown by recent band-structure calculations.[7] Furthermore, the total resistivity would also contain contributions due to mutual scattering of the electrons on the closed nearly spherical part of the Fermi surface as well as their scattering against the electrons of the open scaffold structure. In addition, contributions owing to inelastic processes such as scattering against spin-density fluctuations would have to be considered. The scattering processes involving only the closed nearly spherical part of the Fermi surface would be expected to give rise to a T^2 term in the resistivity. For these reasons the extraction of a $T^2\ln|kT/\mu|$ term in the measured resistivity of Pd does not appear promising.

Although not immediately applicable to a real metal, the result of the preceding calculation does however warn one against assuming that electron-electron interactions invariably contribute a T^2 term to the resistivity regardless of the shape of the Fermi surface. Furthermore if the "cylinder" in question were a long thin elipsoid, then the argument of the logarithm would contain an additional term depending on the radii of curvature of the elipsoid. Hence even though the resistance were still proportional to T^2, its coefficient could be consid-

erably enhanced over conventional estimates. It would be interesting to attempt a calculation using the Golden Rule for other shapes of Fermi surface such as the cubes found in chromium or the cigars of beryllium.

ACKNOWLEDGMENT

Appendix A was written with N. D. Mermin.

APPENDIX A: DENSITY OF STATES AND SUSCEPTIBILITY

It has been observed[4] that the static susceptibility of a noninteracting gas occupying a cylindrical Fermi sea is independent of the wave vector $\vec{q}$ if the component of $\vec{q}$ perpendicular to the cylindrical axis is less than the cylindrical diameter, which we denote $2k_F$. For $q > 2k_F$, the susceptibility decreases. That this result can be uniquely related to the density of states has not been previously noted and is demonstrated here.

The susceptibility function is defined as

$$\chi(\vec{q}) = \sum_{\vec{p}} \frac{f_{\vec{p}+\vec{q}/2} - f_{\vec{p}-\vec{q}/2}}{\epsilon_{\vec{p}-\vec{q}/2} - \epsilon_{\vec{p}+\vec{q}/2}} \tag{A1}$$

$$= \int \frac{d^3p}{(2\pi)^3} \frac{f[(p^2 - \vec{p}\cdot\vec{q} + \frac{1}{4}q^2)(\hbar^2/2m)] - f[(p^2 + \vec{p}\cdot\vec{q} + \frac{1}{4}q^2)(\hbar^2/2m)]}{\hbar^2 \vec{p}\cdot\vec{q}/m} , \tag{A2}$$

since $\epsilon_{\vec{p}} = \hbar^2 p^2/2m$ (in this appendix $\vec{p}$ and $\vec{q}$ denote wave vectors). As usual $f_{\vec{p}}$ is the Fermi function.

We utilize a trick originated by Celli and Mermin[8] to write

$$\chi(\vec{q}) = \int \frac{d^3p}{(2\pi)^3} (-1) \int_{-1}^{1} d\lambda \frac{1}{(\hbar^2 \vec{p}\cdot\vec{q}/m)} \times \frac{\partial}{\partial \lambda} f[(p^2 + \lambda \vec{p}\cdot\vec{q} + \tfrac{1}{4}q^2)\hbar^2/2m] \tag{A3}$$

$$= -\int \frac{d^3p'}{(2\pi)^3} \frac{1}{2} \int_{-1}^{1} d\lambda\, f'\left[\left(p'^2 + \frac{(1-\lambda^2)q^2}{4}\right)\frac{\hbar^2}{2m}\right] . \tag{A4}$$

In (A4) we have changed the momentum variables to $\vec{p}' = \vec{p} + \frac{1}{2}\lambda\vec{q}$. The derivative of the Fermi function with respect to its explicit argument is denoted by f'. At zero temperature we replace it with the negative of a δ function and obtain

$$\chi(\vec{q}) = \frac{1}{2} \int d\epsilon\, N(\epsilon) \int_{-1}^{1} d\lambda\, \delta\left[\epsilon + \frac{\hbar^2 q^2}{2m}\frac{1}{4}(1-\lambda^2) - \mu\right] \tag{A5}$$

$$= \frac{1}{2} \int_{-1}^{1} d\lambda\, N\left[\frac{\hbar^2}{2m}\left(k_F^2 - (1-\lambda^2)q^2/4\right)\right] , \tag{A6}$$

where we have introduced the density of states for a single spin $N(\epsilon)$ and used that the chemical potential is $\mu = \hbar^2 k_F^2/2m$.

The result (A6) is valid for a sphere as well as a cylinder. Specializing to the case of a cylinder of length $L/\hbar$ in wave-vector space we use

$$N(\epsilon) = \text{const} = [m/(2\pi\hbar)^2](L/\hbar), \quad \epsilon > 0$$
$$= 0, \quad \text{otherwise.}$$

The integral (A6) for $\vec{q}$ perpendicular to the axis of the cylinder whose diameter is $2k_F$ becomes

$$\chi(q) = [m/(2\pi\hbar)^2](L/\hbar), \quad q < 2k_F$$

$$= [m/(2\pi\hbar)^2](L/\hbar)\{1 - [1 - (2k_F/q)^2]^{1/2}\}, \quad q > 2k_F. \tag{A7}$$

APPENDIX B

In this appendix we derive the result (5). We remind the reader of the fact that all momenta lie in the same plane perpendicular to the cylinder axis (Fig. 1). The angle $\theta_{1_0'}$ is found using energy conservation

$$p_{2'}^2 + p_{1'}^2 = p_1^2 + p_2^2 \tag{B1}$$

and momentum conservation

$$p_{2'}^2 = (\vec{p}_1 + \vec{p}_2 - \vec{p}_{1'})^2$$
$$= p_1^2 + p_2^2 + p_{1'}^2 + 2p_1p_2\cos\theta_2 - 2p_{1'}p_1\cos\theta_{1'} - 2p_{1'}p_2\cos(\theta_{1'} - \theta_2). \tag{B2}$$

By combining (B1) and (B2) we may write

$$p_{1'}^2 = p_{1'}p_1\cos\theta_{1'} + p_{1'}p_2\cos(\theta_{1'} - \theta_2) - p_1p_2\cos\theta_2$$
$$= \frac{p_{1'}p_2\sin\theta_2}{\cos u}\sin(\theta_{1'} + u) - p_1p_2\cos\theta_2, \tag{B3}$$

where

$$\tan u = \frac{p_1 + p_2\cos\theta_2}{p_2\sin\theta_2} . \tag{B4}$$

From (B2) it follows that

$$\frac{\partial p_{2'}^2}{\partial \theta_{1'}} = 2p_{1'}p_1\sin\theta_{1'} + 2p_{1'}p_2\sin(\theta_{1'} - \theta_2)$$
$$= -2p_{1'}p_2\sin\theta_2\frac{\cos(\theta_{1'} + u)}{\cos u} . \tag{B5}$$

This equation is rewritten as

$$\left|\frac{\partial p_{2'}^2}{\partial \theta_{1'}}\right|_{\theta_{1'}=\theta_{1'0}} = \left(\frac{4p_1^2 p_{1'}^2 p_2^2 \sin^2\theta_2}{\cos^2 u}\cos^2(\theta_{1'}+u)\right)^{1/2}$$
$$= (4p_{1'}^2(p_1^2+p_2^2-p_{1'}^2) - 4p_1^2 p_2^2\cos^2\theta_2)^{1/2}, \quad \text{(B6)}$$

where the latter equality follows from solving (B3) for $\theta_{1'} = \theta_{1'0}$. We always measure energies from the Fermi energy μ. Then (B6) becomes

$$\left|\frac{\partial \epsilon_{2'}}{\partial \theta_{1'}}\right|_{\theta_{1'}=\theta_{1'0}} = 2[(\mu+\epsilon_{1'})(\mu+\epsilon_1+\epsilon_2-\epsilon_{1'}) - (\mu+\epsilon_1)(\mu+\epsilon_2)\cos^2\theta_2]^{1/2}$$
$$= 2(\epsilon_{1'}(\epsilon_1+\epsilon_2-\epsilon_{1'}) - \epsilon_1\epsilon_2 + (\mu+\epsilon_1)(\mu+\epsilon_2)\sin^2\theta_2)^{1/2}. \quad \text{(B7)}$$

The condition that (B3) has a solution $\theta_{1'} = \theta_{1'0}$ is identical to the condition that the quantity beneath the square-root sign in (B8) is positive. This results in the constraint on $\sin\theta_2$ given in the main text.

APPENDIX C

Here we discuss the details of the evaluation of $F(t)$ as given by (12). It is convenient to consider the terms with $\ln|x-z|$ and $\ln|t-x|$ separately. We shall prove that they are in fact identical. In the integral involving $\ln|x-z|$, we make the variable transformation $y = -x+z$, which requires us to evaluate an integral of the form

$$I_1(t) = \int_{-\infty}^{\infty} dx \int_{-\infty}^{\infty} dy \ln|y| \times f(y+x)[1-f(x)][1-f(t+y)]$$
$$= \int_{-\infty}^{\infty} dy \ln|y| \,[y/(e^y-1)][1-f(t+y)], \quad \text{(C1)}$$

by the use of the identity

$$\int_{-\infty}^{\infty} dx f(x+y)[1-f(x)] = y/(e^y-1). \quad \text{(C2)}$$

The term with $\ln|t-x|$ is handled similarly by changing variables to $y = t-x$ and performing the integration over z by means of (C2). The result is seen to be identical to (C1).

The function $F(t)$ is therefore

$$F(t) = [1-f(t)]^{-1}\int_{-\infty}^{\infty} dy \ln|y| \,[y/(e^y-1)](1-f(t+y)] \quad \text{(C3)}$$
$$= \frac{1}{2}\int_0^{\infty} dy \ln y \frac{y}{\sinh\frac{1}{2}y} \times\left(\frac{\cosh\frac{1}{2}t}{\cosh\frac{1}{2}(y-t)} + \frac{\cosh\frac{1}{2}t}{\cosh\frac{1}{2}(y+t)}\right). \quad \text{(C4)}$$

From (C4) one observes that $F(t)$ is even, $F(t) = F(-t)$.

The value of $F(t)$ for $t=0$ can be evaluated analytically.[9] We may write

$$F(0) = 2\int_0^{\infty} dy \frac{y\ln y}{\sinh y}$$
$$= 4\sum_m \int_0^{\infty} dy\, y \ln y\, e^{-y(1+2m)}$$
$$= 4\sum_m \frac{1}{(2m+1)^2}\left[\int_0^{\infty} dy\, y \ln y e^{-y} - \ln(1+2m)\right]$$
$$= 4\times\frac{\pi^2}{8}(1-\gamma) - 4\sum_{m=1}^{\infty}\frac{\ln(1+2m)}{(1+2m)^2}. \quad \text{(C5)}$$

Here γ is Euler's constant, $\gamma = 0.577\,215$. The sum was evaluated to give $F(0) = 0.41\,388$. The integral (C4) has been calculated numerically for $t \neq 0$, and the result is shown in Fig. 2. The numerical calculation gave $F(0) = 0.412$, which compares reasonably with the analytic result (C5).

APPENDIX D

At zero temperature one can easily relate the decay rate of an electron above the Fermi sea to the wave-vector- and frequency-dependent susceptibility function $\chi(\vec{q},\omega)$ defined by

$$\chi(\vec{q},\omega) = \sum_{\vec{p}} \frac{f_{\vec{p}+\vec{q}/2} - f_{\vec{p}-\vec{q}/2}}{\epsilon_{\vec{p}-\vec{q}/2} - \epsilon_{\vec{p}+\vec{q}/2} + \hbar\omega + i\delta}. \quad \text{(D1)}$$

In (D1) $\vec{p}$ and $\vec{q}$ denote wave vectors. At $\omega = 0$ (D1) is identical to $\chi(\vec{q})$ given by (A1).

In order to establish the connection between the decay rate and the susceptibility function (D1) we write Eq. (2) of the main text in the form

$$\frac{1}{\tau(\epsilon_1)} = \frac{2W}{(2\pi)^6}\left(-\frac{1}{\pi}\right)\mathrm{Im}\int d\vec{q}(1-f_{\vec{p}_1-\vec{q}}) \times\int d\vec{p}_2 \frac{f_{\vec{p}_2}(1-f_{\vec{p}_2+\vec{q}})}{\epsilon_{\vec{p}_2} - \epsilon_{\vec{p}_2+\vec{q}} + \epsilon_{\vec{p}_1} - \epsilon_{\vec{p}_1-\vec{q}} + i\delta}. \quad \text{(D2)}$$

We have changed to wave-vector variables and written $\vec{p}_{1'} = \vec{p}_1 - \vec{q}$, $\vec{p}_{2'} = \vec{p}_2 + \vec{q}$ in going from (2) to (D2).

The susceptibility function can be separated as follows:

$$\chi(\vec{q},\omega) = \sum_{\vec{p}_2}\frac{f_{\vec{p}_2+\vec{q}} - f_{\vec{p}_2}}{\epsilon_{\vec{p}_2} - \epsilon_{\vec{p}_2+\vec{q}} + \hbar\omega + i\delta}$$
$$= \sum_{\vec{p}_2}\left[\frac{f_{\vec{p}_2}(1-f_{\vec{p}_2+\vec{q}})}{\epsilon_{\vec{p}_2+\vec{q}} - \epsilon_{\vec{p}_2} + \hbar\omega + i\delta} - \frac{f_{\vec{p}_2}(1-f_{\vec{p}_2+\vec{q}})}{\epsilon_{\vec{p}_2} - \epsilon_{\vec{p}_2+\vec{q}} + \hbar\omega + i\delta}\right]. \quad \text{(D3)}$$

Note that each of the two terms depends on only the magnitude of $\vec{q}$ and not on its direction. At zero temperature the energy difference $(\epsilon_{\vec{p}_2+\vec{q}} - \epsilon_{\vec{p}_2})$ is positive in both terms because of the factor $f_{\vec{p}_2}(1-f_{\vec{p}_2+\vec{q}})$. Therefore, the first term contributes to the imaginary part of χ only for negative frequencies, whereas the second one contributes only for positive frequencies.

At zero temperature the decay rate may therefore be written as

$$\frac{1}{\tau(\epsilon_1)} = \frac{2W}{(2\pi)^3}\frac{1}{\pi}\int' d\vec{q}\,(1-f_{\vec{p}_1-\vec{q}})\,\mathrm{Im}\chi(q, \epsilon_{\vec{p}_1} - \epsilon_{\vec{p}_1-\vec{q}}), \tag{D4}$$

where the prime on the integral sign indicates that the range of $\vec{q}$ is restricted to the region defined by

$$\epsilon_{\vec{p}_1} - \epsilon_{\vec{p}_1-\vec{q}} > 0 .$$

The connection (D4) between the lifetime and the susceptibility is valid for an arbitrary Fermi surface. For the discussion of $\chi(\vec{q}, \omega)$ in specific examples it is convenient to introduce the reduced variables

$$x \equiv q/2k_F \quad \text{and} \quad x_0 \equiv \hbar\omega/4\mu . \tag{D5}$$

According to (D4) the frequency variable ω equals $(1/\hbar)$ times the energy difference $\epsilon_{\vec{p}_1} - \epsilon_{\vec{p}_1-\vec{q}}$. For a sphere or a cylinder of "free" electrons, for which $\epsilon_p = \hbar^2p^2/2m$, with p denoting the magnitude of the transverse wave vector in the cylindrical case and the magnitude of the wave vector itself in the spherical case, we have

$$x_0 = \alpha x_1 x - x^2 , \tag{D6}$$

in terms of the variables

$$\alpha \equiv \cos\varphi = (\vec{p}_1\cdot\vec{q})/p_1 q \tag{D7a}$$

and

$$x_1 \equiv p_1/k_F . \tag{D7b}$$

Here φ is the angle between $\vec{p}_1$ and $\vec{q}$ (it is understood that the wave vectors are transverse to the axis in the cylindrical case).

The restriction to positive frequencies means that $x_0 > 0$ or

$$\alpha x_1 < x . \tag{D8}$$

We may remove the factor $(1-f_{\vec{p}_1-\vec{q}})$ from the integrand of (D4) provided we restrict further the region of the $\vec{q}$ integration by requiring that the scattered electron has an energy greater than the Fermi energy $\mu = \hbar^2k_F^2/2m$, i.e., $\epsilon_{\vec{p}_1-\vec{q}} > \mu$ or equivalently

$$\alpha x_1 < x + (x_1^2 - 1)/4x . \tag{D9}$$

In addition to (D8) and (D9) the range of α is obviously limited by the condition $\alpha < 1$. The resulting region of integration in the x-α plane $S(x, \alpha)$ is shown in Fig. 3 (heavy lines) for the case $x_1 = 1.2$.

We proceed to calculate the imaginary part of the susceptibility for a cylindrical Fermi surface and compare it with the well-known result[10] for a sphere. In both geometries we can utilize the trick which was employed in Appendix A for calculating the static susceptibility. Then for cylindrical geometry (D1) becomes

$$\chi(\vec{q}, \omega) = \int\frac{d^3p}{(2\pi)^3}\,\frac{1}{2}\int_{-1}^{1} d\lambda\tilde{\alpha}\,\frac{f'\{(\hbar^2/2m)(p^2+pq\tilde{\alpha}\lambda+q^2/4)\}}{-\tilde{\alpha}+m\omega/\hbar pq+i\delta}, \tag{D10}$$

where $\tilde{\alpha} = (\vec{p}_\perp\cdot\vec{q})/pq$ and $|\vec{p}_\perp| = p$ (see Fig. 4). At zero temperature $f'(x) = -\delta(x-\mu)$. The imaginary part of (D10) is trivially written down in terms of integrals over the product of two δ functions and $\tilde{\alpha}$. The volume element for d^3p in the cylindrical case is

$$d^3p = p\,dp\,d\tilde{\varphi}\,dp_z , \tag{D11}$$

with $\tilde{\varphi} = \cos^{-1}\tilde{\alpha}$ (see Fig. 4). The integral over the axis of the cylinder whose length is $L/\hbar$ in wave-vector space is trivially performed. Then, where we have used the identifications (D5) and $\epsilon = (p/k_F)^2$, (D10) becomes

$$\mathrm{Im}\chi = \frac{L}{\hbar}\,\frac{1}{(2\pi)^3}\,\frac{\pi}{2}\int_{-1}^{1}d\lambda\int_{-1}^{1}d\tilde{\alpha}\,\frac{1}{(1-\tilde{\alpha}^2)^{1/2}}\left(2\,\frac{m}{\hbar^2}\right)\int_0^\infty d\epsilon\;\tilde{\alpha}\,\delta(\tilde{\alpha}-x_0/x\sqrt{\epsilon})\,\delta(\epsilon+2x\tilde{\alpha}\lambda\sqrt{\epsilon}+x^2-1)$$

$$= \frac{L}{\hbar}\,\frac{1}{8\pi^2}\,\frac{m}{\hbar^2}\int_{-1}^{1}d\lambda\int_{(x_0/x)^2}^{\infty}d\epsilon\,\frac{x_0/x}{[\epsilon-(x_0/x)^2]^{1/2}}\;\delta(\epsilon+2x_0\lambda+x^2-1) . \tag{D12}$$

The ϵ integral is trivially performed to leave an integral over λ between a lower limit (-1) and an upper limit λ_u which is determined by constraints arising naturally from the argument of the δ function and the lower limit of the ϵ integral in (D12). There are two regions in the (x, x_0) space where λ_u is different from (-1), in which case (D12) is zero. These are

case a: $0 < x_0 < x - x^2$, $\quad 0 < x < 1$ (D13a)

case b: $x - x^2 < x_0 < x + x^2$, $\quad 0 < x < 1$

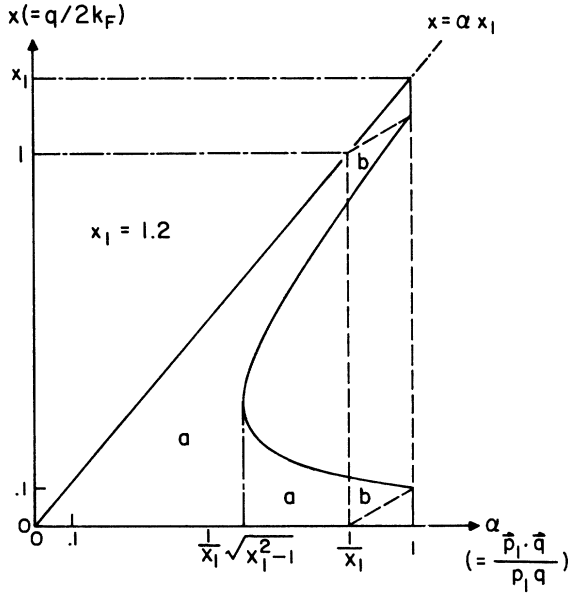

FIG. 3. Regions of integration in the x-α plane for the case where $x_1 \equiv p_1/k_F = 1.2$. The solid lines mark the boundaries of the region $S(x, \alpha)$ defined by (D8), (D9), and $\alpha < 1$. The dashed lines correspond to the regions given by (D18a) and (D18b). Inside the regions marked a and b in the figure the expression (D15a) and (D15b), respectively, should be used for $F(x, x_0(x, \alpha, x_1))$ in (D17). The exact decay rate equals the sum of the contributions from a and b.

$$x^2 - x < x_0 < x + x^2, \qquad x > 1 . \tag{D13b}$$

For these two cases, we have $\lambda_u = 1$ and $[1 - x^2 - (x_0/x)^2]/2x_0$, respectively. The results of λ integral can be expressed as

$$\mathrm{Im}\chi(q, \omega) = \frac{L}{\hbar}\frac{1}{8\pi^2}\frac{m}{\hbar^2} F(x, x_0) , \tag{D14}$$

where

$$F(x, x_0) = \frac{1}{x}\left\{\left[1 - \left(\frac{x_0}{x} - x\right)^2\right]^{1/2} - \left[1 - \left(\frac{x_0}{x} + x\right)^2\right]^{1/2}\right\},$$

case a (D15a)

and

$$F(x, x_0) = \frac{1}{x}\left[1 - \left(\frac{x_0}{x} - x\right)^2\right]^{1/2}, \qquad \text{case b} .$$

(D15b)

We note that $F(x, x_0)$ is zero for all parts of upper right-hand quadrant of (x, x_0) space not included in cases a and b.

The calculation of the imaginary part of the susceptibility can be calculated for a *spherical* Fermi surface in a similar fashion. We find that

$$\mathrm{Im}\chi(q, \omega) = \frac{k_F}{16\pi}\frac{m}{\hbar^2} G(x, x_0) , \tag{D16}$$

where $G(x, x_0)$ is simply obtained from (D15) by replacing all square-root signs with parentheses. Thus, for case a, $G(x, x_0) = 4x_0/x$.

We now proceed to calculate the lifetime for the cylindrical case. As discussed earlier [see Eqs. (D8) and (D9)] we obtain the lifetime by integrating $\mathrm{Im}\chi$ over a certain region $S(x, \alpha)$ in the x-α plane. Apart from a numerical constant the energy dependence of the inverse lifetime or decay rate is therefore given by the x_1 dependence of the integral

$$I = \int_{S(x,\alpha)} x\,dx \int \frac{d\alpha}{(1-\alpha^2)^{1/2}} F(x, x_0(x, \alpha, x_1)) , \tag{D17}$$

where x_0 is given by (D6) and x_1 defined in (D7b). The region $S(x, \alpha)$ is defined by (D8) and (D9) together with the condition $\alpha < 1$. The fact that $F(x, x_0)$ is nonzero only in the region given by (D 13a) and (D13b) has the effect of diminishing the integration to two regions with $S(x, \alpha)$. These are

$$\text{case a:} \quad 0 < x < \alpha x_1, \quad 0 < \alpha x_1 < 1 \tag{D18a}$$

where $F(x, x_0(x, \alpha, x_1))$ is (D15a), and

$$\text{case b:} \quad \tfrac{1}{2}(\alpha x_1 - 1) < x < \tfrac{1}{2}(1 + \alpha x_1), \quad 1 < \alpha x_1 < x_1 \tag{D18b}$$

where $F(x, x_0(x, \alpha, x_1))$ is (D15b). Insofar as the boundaries of these regions in the $x - \alpha$ plane differ from those of $S(x, \alpha)$ they are marked with a dashed line in Fig. 3. We observe that there are two small triangular regions of $S(x, \alpha)$ where F

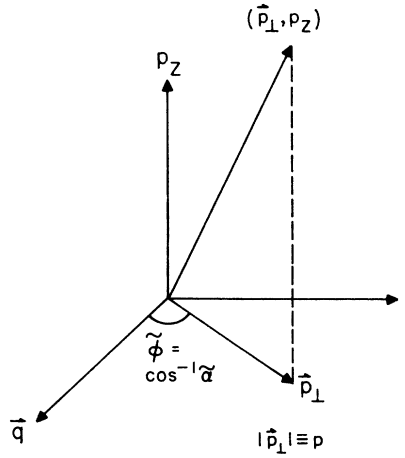

FIG. 4. In the cylindrical case the wave vector $\vec{q}$ is perpendicular to the axis and $\tilde{\phi}$ is the azimuthal angle with respect to it as indicated in the figure and in (D11). The magnitude $|\vec{p}_\perp|$ of the transverse wave-vector component is the p of (D11).

is zero.

The remainder of the job in calculating the decay rate is to evaluate (D17) in those parts of the regions (D18a) and (D18b) that lie inside $S(x, \alpha)$ with $F(x, x_0(x, \alpha, x_1))$ given by (D15a) and (D15b), respectively. Here we shall only consider the dominant term in $1/\tau(\epsilon_1)$ for small values of the parameter ϵ defined by

$$\epsilon \equiv (\epsilon_{\vec{p}_1} - \mu)/\mu = x_1^2 - 1. \tag{D19}$$

The contribution to the integral I in (D17) from the regions marked (b) in Fig. 3 [corresponding to region (D18b)] is then negligible compared to the contribution from the region marked (D18a). With (D15a) in (D17) one gets from the integration over x

$$\int x\,dx\,F(x, x_0(x, \alpha, x_1)) = \tfrac{1}{4}(2x - \alpha x_1)\,[1 - (\alpha x_1 - 2x)^2]^{1/2} + \tfrac{1}{4}\sin^{-1}(2x - \alpha x_1) - x(1 - \alpha^2 x_1^2)^{1/2}\,. \tag{D20}$$

When $\alpha x_1 < [x_1^2 - 1]^{1/2} = \epsilon^{1/2}$ the proper limits on x to be inserted in (D20) are given by $0 < x < \alpha x_1$ (compare Fig. 3). The contribution of this region to $1/\tau(\epsilon_1)$ results in a leading term which goes as ϵ^2.

The dominant $\epsilon^2|\ln\epsilon|$ dependence is obtained from the contribution to (D17) in the region $\epsilon^{1/2} < \alpha x_1 < 1$ (see Fig. 3). When the proper limits on x derived from (D8) and (D9) are inserted in (D20) the integral (D17) becomes

$$I = \frac{1}{(1+\epsilon)^{1/2}} \int_{\epsilon^{1/2}}^{1} dy \times \Big((1-y)^{1/2}(y^2-\epsilon)^{1/2} - \tfrac{1}{2}(1+\epsilon-y)^{1/2}(y^2-\epsilon)^{1/2} - (1-y^2)^{1/2} y + \tfrac{1}{2}\sin^{-1} y - \tfrac{1}{2}\sin^{-1}(y^2-\epsilon)^{1/2} \times \frac{1}{(1+\epsilon-y^2)^{1/2}} \Big)\,, \tag{D21}$$

where $y \equiv \alpha x_1$ and x_1 has everywhere been replaced by $(1+\epsilon)^{1/2}$.

Since we were unable to perform all the integrals in (D21) analytically the integrand was expanded for small values of y ($y \ll 1$, $\epsilon^{1/2} \ll 1$) where one would expect the dominant $\epsilon^2 \ln\epsilon$ term to appear. The contribution to I from the lower limit was found to be

$$I = -\tfrac{1}{16}\epsilon^2 \ln\epsilon + O(\epsilon^2)\,.$$

With (D22) and (D14) the decay rate (D4) finally becomes

$$\frac{1}{\tau(\epsilon)} = \frac{2}{(2\pi\hbar)^6}\, W m^2 L^2 \mu (-\epsilon^2 \ln\epsilon)\,, \tag{D23}$$

which is identical to the leading term of (17). The treatment given here also exhibits the importance of the region of small momentum transfer (small $x = q/2k_F$), since the $\epsilon^2 \ln\epsilon$ term appeared as the contribution from the lower limit $\epsilon^{1/2}$ in (D21) where x is also small (Fig. 3). If the transition probability W is assumed to depend on q (and hence x) instead of being a constant as previously assumed, the $\epsilon^2 \ln\epsilon$ behavior would persist provided W depends weakly on x for small values of x.

The calculation of the decay rate for a sphere goes through in the same manner. All the integrals may be performed analytically in the various regions in Fig. 3, when a constant transition probability W is assumed. Upon expansion of the result in powers of ϵ we get

$$\frac{1}{\tau(\epsilon)} = \frac{m^3 W}{(8\hbar^6\pi^4)}\, \mu^2 \epsilon^2 [1 - \tfrac{2}{3}\epsilon + O(\epsilon^2)]\,. \tag{D24}$$

The quadratic term of (D24) is just the well-known (approximate) expression for the decay rate (see, e.g., Ref. 2) which may be obtained in the manner of Abrikosov and Khalatnikov.[11]

The magnitude of the ϵ^3 term gives an indication of the degree to which Abrikosov and Khalatnikov's[11] approximate transformation of the Boltzmann equation of a Fermi liquid should be trusted. To our knowledge such correction terms have not previously been determined.

If the transition probability here is assumed to depend on $x(= q/2k_F)$ the quadratic term in ϵ that appears in (D24) is unchanged except for the replacement of W with the average $\int_0^1 W(x)\,dx$. The ϵ^3 and higher terms, however, are affected by the details of the momentum dependence of $W(x)$.

---

*Work supported in part by the National Science Foundation under Grant No. GP-27355, in part by the Advanced Research Projects Agency through the Materials Science Center at Cornell University, MSC Report No. 1471, and in part by Statens Teknisk-Videnskabelige Fond, Denmark.

†Alfred P. Sloan Foundation Fellow.

[1]J. C. Garland and R. Bowers, Phys. Rev. Letters 21, 1007 (1968); J. T. Schriempf, A. I. Schindler, and D. L. Mills, Phys. Rev. 187, 959 (1969), and references therein.

[2]See, for example, D. Pines and P. Nozières, *The Theory of Quantum Liquids*, Vol. I (Benjamin, New York, 1969), p. 61ff.

[3]See, e.g., J. Ziman, *Electrons and Phonons* (Oxford U. P., New York, 1960), p. 415.

[4]J. R. Schrieffer, Phys. Rev. Letters 19, 644 (1967).

[5]Strictly speaking, W has to depend only on the momentum transfer perpendicular to the cylinder axis for this result to be valid. However, as long as W is only a weak function of the momenta involved in the collision, it is

reasonable to believe that the energy and temperature dependence of the decay rate will be essentially the same as the one we calculate assuming W is a constant.

[6]C. Herring, Phys. Rev. Letters 19, 167, (1967); 19, 684(E) (1967).

[7]Ole Krogh Andersen, Phys. Rev. B 2, 883 (1970).

[8]V. Celli and N. D. Mermin, Phys. Rev. 140, A839 (1965).

[9]The authors are grateful to J. P. Straley for spontaneously performing the calculation of $F(0)$ described in the text.

[10]J. Lindhard, Kgl. Danske Videnskab. Selskab, Mat.-Fys. Medd. 28, No. 8 (1954).

[11]A. A. Abrikosov and I. M. Khalatnikov, Rept. Progr. Phys. 22, 329 (1959).

PHYSICAL REVIEW B VOLUME 4, NUMBER 2 15 JULY 1971

Radio-Frequency Size Effect and the Fermi Surface of Molybdenum†

J. R. Cleveland* and J. L. Stanford
Institute for Atomic Research and Department of Physics, Iowa State University, Ames, Iowa 50010

(Received 28 September 1970; revised manuscript received 29 March 1971)

Fermi-surface dimensions for the (110) plane for molybdenum are determined from caliper dimensions obtained through radio-frequency size-effect measurements. These measurements were taken over a frequency range of 6.5–26 MHz on high-purity molybdenum approximately 0.13 mm in thickness. Studies of the frequency dependence of the extrema in the resonance line shape were used to determine the magnetic field values for resonances along major crystallographic directions. The Fermi-surface dimensions are compared with recent theoretical and experimental work on molybdenum.

I. INTRODUCTION

The Fermi surface and energy-band structure of molybdenum have been the subjects of several investigations in recent years. The Fermi-surface model for Mo was first proposed by Lomer.[1] In a subsequent augmented-plane-wave (APW) calculation Loucks[2] determined Fermi-surface dimensions along the major symmetry directions, which verified the Lomer model. However, a detailed calculation of the Mo band structure and Fermi surface has not been published. Experimental studies of the Mo Fermi surface have been reported on the anomalous skin effect,[3] the dc size effect,[4] the magnetoresistance,[5,6] the de Haas–van Alphen (dHvA) effect,[7–10] the magnetoacoustic effect,[11,12] cyclotron resonance,[13] and the radio-frequency size effect (RFSE).[14,15] In the present publication we present the results of a RFSE investigation on the (110) plane in Mo in which the resonance field values were determined on the basis of frequency studies of the RFSE line shapes. A preliminary report of this work has been given.[16] Reviews of the experimental aspects of the RFSE technique have been written by Gantmakher[17] and by Walsh.[18] The theoretical aspects are discussed in a review by Kaner and Gantmakher[19] and in recent papers by Juras.[20,21] In RFSE experiments, a flat single-crystal metal plate, sufficiently pure that the electron mean free path is on the order of the thickness of the plate at helium temperatures, is placed in the presence of a magnetic field. For electrons executing trajectories such that $\vec{v}\cdot\vec{n}=0$ ($\vec{v}$ is electron velocity and $\vec{n}$ is normal to plate surfaces) at the two surfaces of the plate, anomalies (RFSE resonances) occur in the surface impedance of the plate. For the magnetic field directed parallel to the plate surfaces, these anomalies yield Fermi-surface caliper dimensions $|\Delta\vec{k}|$ given by $\Delta\vec{k}=(e/\hbar)t(\vec{n}\times\vec{B}_{res})$, where t is the sample thickness and B_{res} is the magnetic field value at the resonance. For central orbits $\Delta\vec{k}=2\vec{k}_F$.

Because the RFSE resonance linewidth ΔH extends over a field range 5–20% of the magnetic field magnitude, the assignment of accurate resonance field values is difficult. The question therefore arises as to what are the proper criteria to use to determine the correct resonance field value. In an investigation on potassium, Koch and Wagner[22] assigned B_{res} to a point close to the first discernible departure of the resonance from the background. This assignment was made on the basis of a study of the frequency dependence of the linewidth and from the known Fermi-surface dimensions for potassium. Krylov and Gantmakher[23] found in a similar study on In that the resonance linewidth reduced to zero with extrapolation to infinite frequency at a field value corresponding to a position quite close to the low-field side of the resonance. They concluded that the field value obtained with this technique is the proper value to assign to the resonance. A result similar to that of Krylov and Gantmakher was obtained by the present authors.[16] In all three